

J.L. GAO^{1,✉,*}
C.N. NG²

Deconvolution filtering of ground-based LIDAR returns from tropospheric aerosols

¹ Department of Physics and Materials Science, City University of Hong Kong, Kowloon, Hong Kong

² Department of Geography and Geology, University of Hong Kong, Pokfulam Road, Hong Kong

Received: 8 October 2002 / Revised version: 29 January 2003
Published online: 22 May 2003 • © Springer-Verlag 2003

ABSTRACT A deconvolution filtering model of multiple scattering in ground-based single field of view (SFOV) LIDAR returns is described. It is based on time series deconvolution techniques. The contribution of multiply scattered photons in SFOV LIDAR returns can be numerically modeled by processing LIDAR signals without additional information about aerosol properties and measurement geometry. Deconvolution results are in good agreement with those performed by Monte Carlo calculations, showing that the significance of multiply scattered photons is strongly correlated with aerosol concentration. It is found that, for ground-based LIDAR, the contribution of multiply scattered photons to LIDAR signals is typically below 5% in a clear urban atmosphere, and up to 14% in a very dirty urban atmosphere in Hong Kong during winter seasons.

PACS 42.68.Wt; 42.79.Qx

1 Introduction

LIDAR backscattered signals are basically a combination of singly scattered signals, multiply scattered signals, and other stochastic disturbances. Calculating the significance of multiple scattering in LIDAR signals is a major point of interest in the recent literature [1–3]. In LIDAR research, as most inversion schemes for deriving extinction coefficients are based on the classical LIDAR equation in which the contribution of multiple scattering is not accounted for, the inversion might be imperfect in some situations such as in high aerosol optical thickness. As pointed out in [4], even for low aerosol optical thickness, the influence of multiple scattering for a space-borne LIDAR is large because of the large volume of the receiver cone.

Various methods have been developed to calculate the significance of multiple scattering in LIDAR measurements from cloud-based atmospheres. A collection of these models and comparative studies can be found in [3], which included the following categories: numerical Monte Carlo simulation, stochastic description of photon scattering, solution of

Maxwell's equations, and approximations to the radiative transfer equation. These studies mainly highlighted situations in which the optical thickness was expected to be high: scattering in clouds or measuring from space. For studies of tropospheric aerosols by a ground-based LIDAR, it is not possible to simply extrapolate those conclusions of cloud studies since the angular distribution for aerosols might be considerably different from clouds, and the ground-based LIDAR normally presents very small field of view (FOV) apertures.

In the case of measuring tropospheric aerosols by a ground-based LIDAR, one can use a Monte Carlo simulation method to investigate multiple scattering in LIDAR returns, but one has to model explicitly the aerosol properties and the specific measurement geometry [5, 6]. Another study of ground-based LIDAR measurements was published by Hutt et al. [7], who developed ground-based multiple field of view (MFOV) LIDAR systems to measure LIDAR returns simultaneously with four concentric FOV receivers. As scattering by aerosols causes the laser-pulse profile to broaden, multiply scattered photons could be received by the outer receiver.

However, the relevance of multiple scattering in the most frequent measurement situation, a ground-based single field of view (SFOV) LIDAR and LIDAR returns influenced by tropospheric aerosols whose properties and measurement geometry are unknown, has not been studied.

This paper describes a numerical model based on time-series techniques applicable to the calculation of multiple scattering from ground-based SFOV LIDAR returns without the need for any supplementary information about aerosol properties and measurement geometry. The results from this model appear to agree with those obtained by Monte Carlo simulations.

2 Proposed model

2.1 Time-series model for LIDAR returns

Every LIDAR measurement is more or less affected by multiply scattered photons since a LIDAR detector collects all photons independent of their numbers of scattering events. In addition, because the multiple-scattered component of the LIDAR signal is depolarized, the depolarization caused by multiple scattering and single scattering from non-spherical particles might also play a role in return signals in some circumstances. A few recent studies have been done

✉ Fax: +81-298/51-8229, E-mail: gao@proteo.gr.jp

*Present address: Preteomics Lab., Amakubo 1-16-1, Tsukuba 305-0005, Japan

to estimate the contribution of multiple scattering by measuring the depolarization ratio using a MFOV LIDAR [7] or by calculating the rotational Stokes vector/Mueller matrix in Monte Carlo simulations [8, 9]. The influences of depolarization in the return signals cannot be discriminated exactly in the framework of the present time-series model since the depolarized signal is not a time series independent of the multiple-scattering signals. Due to lack of prior knowledge of the spectrum and statistics of the atmospheric returns, we concentrate here mainly on the multiple-scattering problems in ground-based LIDAR signals.

In practice, laser scattering in aerosol media is a multiple-path problem. Within the volume of a LIDAR receiver cone, the scattering events occur at different angles, making scattered photons reach the LIDAR receiver along different paths. As FOVs of ground-based LIDAR are very small, directly backscattered photons (i.e. singly scattered photons) travel approximately parallel with the forward direction; a portion of multiply scattered photons produced by the same laser pulse could be scattered to the LIDAR receiver at delayed times according to their numbers of scattering events. In other words, at moment t , the LIDAR detector collects not only singly scattered photons from a laser pulse emitted at instant t but also multiply scattered photons from laser pulses emitted at instants $t - \tau$, $t - 2\tau$, ..., $t - m\tau$, where τ is a lag determined by the scattering path traveled by scattered photons and m is an integer. For simplicity of exposition, we discuss the model of LIDAR returns for $\tau = 1$ in the present paper and the LIDAR returns have the form of the following convolution:

$$Y_t = \sum_{k=0}^m h_k X_{t-k}, \quad (1)$$

where Y_t represents the LIDAR returns, X_{t-k} is the energy of multiple-scattering photons following the k th scattering path, and h_k is the attenuation factor for each scattering event. Clearly, X_t refers to the intensity of singly scattered photons and the summation $\sum_{k=1}^m h_k X_{t-k}$ describes the total intensity of multiply scattered photons. Because it is not possible to keep multiply scattered photons from being detected by the LIDAR receiver, a mathematical description and evaluation of the LIDAR signals on the basis of singly scattered photons alone must be erroneous. It is also not reasonable simply to take the very first part of the signal for each distance to avoid the multiple-scattering problem, since the convolution might occur at each distance. Consequently, the only way of using a time-series approach to estimate multiple-scattering components in LIDAR returns is to solve the convolution model (1).

From the time-series point of view, after the removal of the trend component, the LIDAR returns can be treated as a stochastic time series, which can be written as an autoregressive (AR) process:

$$Y_t + \varphi_1 Y_{t-1} + \varphi_2 Y_{t-2} + \cdots + \varphi_s Y_{t-s} = \theta_0 \varepsilon_t, \quad (2)$$

where φ_s is the regressive coefficient, ε_t and Y_t are mutually independent time series, and ε_t is a standard white-noise series with $E \varepsilon_t = 0$ and $E \varepsilon_t \varepsilon_s = \delta_{t,s}$. For this reason, Y_t denotes

LIDAR returns without a trend component in the present discussion.

Equations (1) and (2) constitute the convolution model of multiple-scattering events, and multiple-scattering items can be numerically calculated by the following deconvolution filtering techniques.

2.2 Deconvolution filtering

On one hand, according to [10], the regressive coefficient, φ_s , can be estimated by the following Yale–Walker equation:

$$\begin{bmatrix} r_0 & r_1 & r_2 & \cdots & r_s \\ r_1 & r_0 & r_1 & \cdots & r_{s-1} \\ \cdots & & & & \\ r_s & r_{s-1} & r_{s-2} & \cdots & r_0 \end{bmatrix} \begin{bmatrix} 1 \\ \varphi_1^s \\ \cdots \\ \varphi_s^s \end{bmatrix} = \begin{bmatrix} \theta_0^s(s) \\ 0 \\ \cdots \\ 0 \end{bmatrix}, \quad (3)$$

where r_s is an auto-correlation function of Y_t , and the order s should be selected as the value which minimizes the AIC index

$$\text{AIC}(s) = \log \theta_0^2 + 2 \frac{S}{N}, \quad (4)$$

where N is the number of samples in one laser pulse.

On the other hand, an AR process can be expressed in its transmitting form such that

$$Y_t = C(B) \varepsilon_t, \quad (5)$$

where

$$\varepsilon_t = [\varphi(B)/\theta_0] Y_t. \quad (6)$$

Here the phase-shift polynomial, $C(B)$, is known as the Green function that takes the form

$$C(B) = \sum_{j=0}^{\infty} C_j B^j, \quad B^j(X_t) = X_{t-j}, \quad (7)$$

where B is the backward-shift operator.

Substituting the signals formulated with Green functions in (2), we have

$$\begin{cases} C_0 = \theta_0, \\ C_1 = -\varphi_1 C_0, \\ C_2 = -\varphi_1 C_1 - \varphi_2 C_0, \\ \cdots \\ C_p = -\varphi_1 C_{p-1} - \varphi_2 C_{p-2} - \cdots - \varphi_p C_0, \\ C_l = -\sum_{s=1}^p \varphi_s C_{l-s}, \quad l > p. \end{cases} \quad (8)$$

Bearing this result in mind, we assume that the multiple-scattering items, X_t , can also be expressed by their Green-function form summed with the standard white-noise series, ε_t , such that

$$X_t = \sum_{l=0}^{\infty} \theta_l \varepsilon_{t-l}. \quad (9)$$

In this manner, the right-hand side of (1) can be rewritten as

$$\begin{aligned}
 Y_t &= \sum_{k=0}^m h_k \left(\sum_{l=0}^L \theta_l \varepsilon_{t-l-k} \right) = \sum_{k=0}^m \sum_{l=0}^L h_k \theta_l \varepsilon_{t-(l+k)} \\
 &= \sum_{l=0}^L \sum_{s=l}^{m+L} h_{s-l} \theta_l \varepsilon_{t-s} = \sum_{s=0}^{m+L} \eta_s \varepsilon_{t-s}, \tag{10}
 \end{aligned}$$

where L is selected by the analyst and

$$\eta_s = \begin{cases} \sum_{l=0}^s \theta_l h_{s-l}, & 0 \leq s \leq m, \\ \sum_{l=0}^L \theta_l h_{s-l}, & M \leq s \leq L, \\ \sum_{l=s-M}^s \theta_l h_{s-l}, & L \leq s \leq L+m. \end{cases} \tag{11}$$

Referring to (8), since a given AR process has only a unique expression of the Green function, we have

$$\begin{cases} C_0 &= \theta_0 h_0, \\ C_1 &= h_1 \theta_0 + h_0 \theta_1, \\ \dots & \\ C_L &= h_L \theta_0 + h_{L-1} \theta_1 + \dots + h_0 \theta_L, \\ C_{L+1} &= h_{L+1} \theta_0 + h_L \theta_1 + \dots + h_1 \theta_L, \\ \dots & \\ C_{L+m} &= h_m \theta_L. \end{cases} \tag{12}$$

Here the total number of unknown parameters in (12) is $L + m + 2$, where the number of equations appearing in (12) is $L + m + 1$. However, to solve (12), we introduce a hypothesis such that (1) is a low-pass filter or, mathematically, $H(\omega) = 1$ if $\omega = 0$, where $H(\omega)$ is the frequency response function of h . That is,

$$\sum_{k=0}^m h_k = 1. \tag{13}$$

This is a reasonable hypothesis since the real signals in LIDAR returns tend to be low-frequency components. Therefore, on account of (13), both the number of unknowns and equations for the model in (12) and (13) are equal to $L + m + 2$, and there might be at least one real solution.

There are, of course, various algorithms that can be used to solve non-linear equations (12) and (13); for example, the Newton hill-climbing scheme [11] or the Newton-Raphson relaxation technique [12]. We preferred the former in this paper to estimate one group of the real solutions for (12) and (13).

The multiple-scattering items, X_t , can be decomposed if the attenuation factors, h_k , have been identified by the iteration of the Newton hill-climbing scheme from (12) and (13). In other words, if the coefficients of a polynomial $H(B)$ are one of the real solutions of (12) and (13), (1) can be rewritten as

$$Y_t = H(B) X_t \tag{14}$$

or, conversely,

$$\begin{aligned}
 X_t &= \frac{1}{H(B)} Y_t \\
 &= \sum_{s=0}^{\infty} d_s Y_{t-s}, \quad t = 0, 1, 2, \dots, \tag{15}
 \end{aligned}$$

where d_s is the deconvolution coefficient for multiple-scattering items.

Expanding (15), all the deconvolution coefficients are given by

$$\begin{cases} d_0 &= \frac{1}{h_0}, \\ d_s &= -\frac{1}{h_0} \sum_{j=0}^{s-1} d_j h_{s-j}, \quad 1 \leq s \leq m, \\ d_s &= -\frac{1}{h_0} \sum_{j=s-m}^{s-1} d_j h_{s-j}, \quad m < s. \end{cases} \tag{16}$$

Thus, multiple-scattering signals, X_{t-k} , could be decomposed from LIDAR returns by following (15).

3 Results and discussion

3.1 Contribution of multiple scattering calculated by deconvolution model

A case study of the contribution of multiple scattering in LIDAR returns is shown in Fig. 1. The calculation was made by (15) for $m = 1, 4, 7$, and 10 while $L = 5, 5, 7$, and 8 , respectively. The selection of L makes no significant difference to the calculations since, by a suitable choice of L , we can always find an approximate solution to (12) and (13).

The contributions of multiply scattered photons at the top of the mixing layer are 8.2%, 12%, 13.2%, and 14%, calculated for $m = 1, 4, 7$, and 10 , respectively. The contribution from the scattering item X_{t-1} dominates in the total contribution made by all multiple-scattering events; the larger m , the less increment of contribution it makes. This is because the scattering item X_{t-m} with a smaller m refers to those photons that traveled closer to directly backscattered signals. These photons are more likely caused by scattering events at smaller

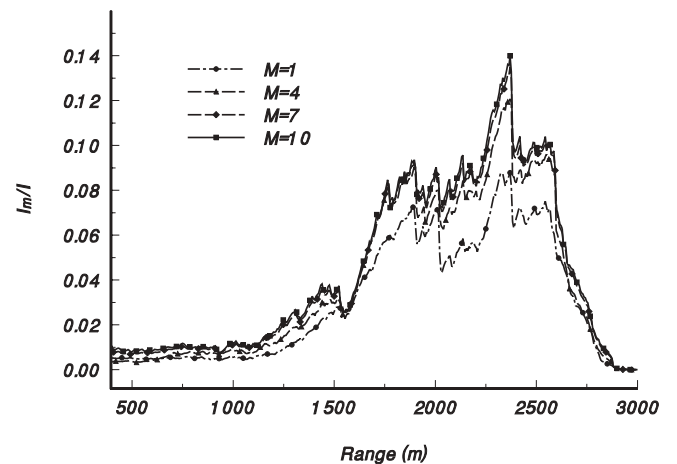


FIGURE 1 Contribution of multiply scattered photons to LIDAR returns calculated by the deconvolution model for $m = 1, 4, 7$, and 10 , respectively

scattering angles near the forward direction. Thus, they have a higher probability of remaining within the FOV of the LIDAR receiver, enhancing the multiply scattered component of the LIDAR signals. There are no significant differences between $m = 7$ and 10 in the calculated profiles. In the deconvolution model (1), for a given m , at the most there are m scattered events accounted for. However, for a small SFOV ground-based LIDAR system and small optical thickness, there are only approximately eight scattering events including the single-scattering event at the most, as LIDAR systems cannot penetrate beyond an optical thickness of 4 [13]. Therefore, $m \leq 7$ is appropriate for the model (1) if it is used for analyzing ground-based LIDAR returns.

Figure 2 shows examples of multiple-scattering effects in several slant-scanned LIDAR measurements. These measurements were made by a SFOV LIDAR using a Nd:YAG laser with an emitted wavelength of 532 nm and a beam divergence of 1 mrad at City University of Hong Kong. The LIDAR system is monostatic and coaxial, and the full angle of the receiver field of view is 2.4 mrad. All the data were collected in wintertime, when the aerosol optical thickness in the urban atmosphere was higher than that in summer in Hong Kong urban areas. In order to analyze contributions of multiply scattered photons for different aerosol optical thicknesses, the selected LIDAR returns represent three typical weather conditions: urban clear atmosphere, urban hazy atmosphere, and urban heavy smoky atmosphere, with approximate visibilities of 5 km, 2 km, and 1 km, respectively.

These measurements have been made at an elevation angle of 17° , and the data in the first 400 m are omitted as a blind zone of the single-pulsed LIDAR. All the calculations are carried out by a Pentium-III PC for $m = 7$.

The contributions of multiply scattered photons are approximately 4%, 8%, and 14% at the top of the mixing layer in urban clear atmosphere, urban hazy atmosphere, and urban heavy smoky atmosphere, respectively. In the urban clear atmosphere, the contribution of multiple scattering is less than one-third of that in the urban heavy smoky atmosphere, showing that the contribution of multiply scattered photons is strongly correlated with the aerosol optical thickness. In add-

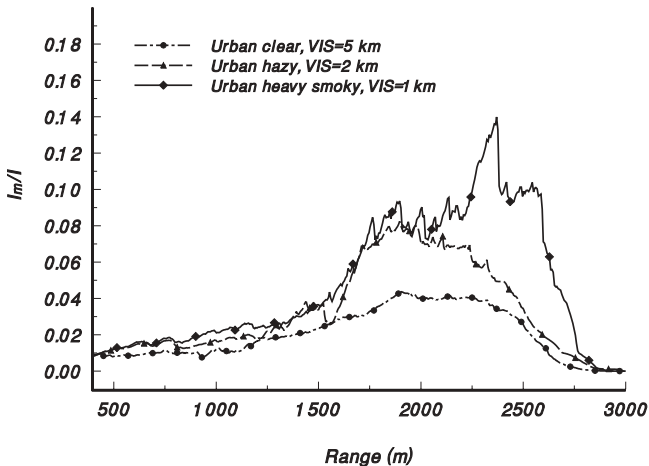


FIGURE 2 Contribution of multiply scattered photons to LIDAR returns calculated by the deconvolution model for urban clear, urban hazy, and urban heavy smoke weather conditions

ition, for a ground-based SFOV LIDAR, the contribution of multiple scattering in a clear atmosphere is really insignificant. Here we should pay more attention to the situation in the urban heavy smoky atmosphere, as the contribution of multiple scatterings is fairly large, even reaching about 14% if eight scattering components are under consideration. This result provides evidence showing that if the aerosol optical thickness is great in the investigated atmosphere, the multiple-scattering signals could be very strong even if they were collected by a ground-based SFOV LIDAR. In this situation, the inversion algorithm based on the single-scattering regime is very imperfect, as multiple scattering is expected to be more important.

3.2 Comparison with Monte Carlo results

As a comparative study, a Monte Carlo simulation has been used in the present paper for the described weather conditions. The simulated LIDAR signals are inverted with and without multiply scattered photons. This allows us to estimate directly the influence of multiple scattering on the retrieval of aerosol-extinction profiles. For a single-scattering event, the LIDAR equation can be written as follows:

$$N_{ss}(r) = CN_0 r^{-2} \times [\sigma_a S_a^{-1}(r) + \beta_m(r)] \exp \left\{ -2 \int_0^r [\sigma_a + \sigma_m] dr \right\}, \quad (17)$$

where $N_{ss}(r)$ is the number of singly scattered photons per sampling-time interval backscattered to the receiver from the distance r , C is an instrumental constant, and subscripts a and m denote aerosols and molecules, respectively. The aerosol extinction-to-backscatter ratio, S_a , is range-dependent, and follows Klett's definition [14], i.e.

$$S_a(r) = \frac{\sigma_a(r)}{\beta_a(r)}, \quad (18)$$

where $\sigma(r)$ and $\beta(r)$ are the extinction coefficient and the backscattering coefficient, respectively.

Alternatively, to account for multiple scattering in the LIDAR equation, a multiple-scattering factor, $\eta(r)$, which is introduced by Platt [1], is used. For the two-component (i.e. aerosol and air molecules) atmosphere, the LIDAR equation including multiply scattered photons reads

$$N_{ss}(r) + N_{ms}(r) = CN_0 r^{-2} \times [\eta(r)\sigma_a S_a^{-1}(r) + \beta_m(r)] \exp \left\{ -2 \int_0^r [\eta(r)\sigma_a + \sigma_m] dr \right\}, \quad (19)$$

where $N_{ms}(r)$ is the number of multiply scattered photons. Accordingly, the result of this inversion is $\eta(r)\sigma_a$ instead of σ_a . Thus, from the inversion of the single-scatter LIDAR equation with and without multiply scattered photons, we obtain the multiple-scattering factor $\eta(r)$ directly by comparing the retrieved aerosol-extinction profiles.

The property of an urban aerosol is taken from Hess et al. [15]. The single-scattering albedo ω_0 and the Mueller matrices that are required for the signal simulations, as well as

the LIDAR ratios for the inversion, are calculated with Mie theory [16] for the wavelength of 532 nm.

A horizontally homogeneous model atmosphere between $r = 0$ km and $r = 4$ km is considered. Within a well-mixed planetary boundary layer (PBL) of 1.5-km thickness, the aerosol-extinction coefficients are assumed to be constant. Values of σ_a are selected as 3.91 km^{-1} , 1.96 km^{-1} , and $7.83 \times 10^{-1} \text{ km}^{-1}$ referring to the visibilities of 1 km, 2 km, and 5 km, respectively [17]. Above the PBL, the particle concentration is assumed to decrease exponentially reaching $\sigma_a = 2.79 \times 10^{-2} \text{ km}^{-1}$ at 2 km and $\sigma_a = 1.14 \times 10^{-2} \text{ km}^{-1}$ at 4 km. More details of this model can be found in [6].

Monte Carlo simulation results of multiple-scattering profiles are presented in Fig. 3. Each calculation is performed with $N_0 = 10^8$ photons, corresponding to a computation time of 60 h on a Pentium-compatible PC with at least 32 Mbytes of RAM. Since measurement geometries and aerosol properties used in this simulation case might not describe the situation of practical atmospheres precisely, shapes of these profiles are different from those calculated by the deconvolution model. However, values of the contribution of multiple scattering in Fig. 3 are quite similar to those exhibited in Fig. 2. For urban clear atmosphere, the contribution is not significant, even below 5%; for urban hazy and urban heavy smoke atmospheres, it reaches approximately 12% and 17.5%, which is 4% and 3% above the values obtained by the deconvolution model, respectively. The simulated result shows that, even for ground-based SFOV LIDAR, the contribution of multiple scattering can be very high in optically thick atmospheres. As a result, such comparisons suggest that the deconvolution filtering model is applicable to analyze multiple-scattering problems in ground-based SFOV LIDAR.

3.3 Relationship between multiple scattering and aerosol concentrations

Analyses of multiple scattering in ground-based LIDAR are quite useful to study air pollution in the local atmosphere, since the influence of multiple scattering is related not only to aerosol properties and measurement geometries but also to the aerosol concentration. In the Hong Kong at-

mosphere during wintertime, air pollutants are in two major categories: particulate matter and gaseous pollutants. The airborne particulate matter is probably the more visible and obvious. It may consist of smoke, dust, fly ash, or condensing vapors. Unlike the heavier particles, the finer particulates can remain airborne for a longer period of time, representing a potential health hazard. Very fine particulates known as respirable suspended particulate (RSP) and fine suspended particulate (FSP), whose size is 10 microns or less and $2.5 \mu\text{m}$ or less, respectively, are the main aerosol matter buoyed in the local atmosphere during wintertime.

The Environmental Protection Department (EPD) of the Hong Kong government has set up different instruments to measure aerosol concentrations over the Hong Kong area. A comparison between concentrations of RSP and FSP observed by EPD and the contribution of multiple scattering in LIDAR returns has been made. The daily observation of particulate concentration and LIDAR sampling were made at 1400 LT for a period of ten days in December 1998. The concentrations of RSP and FSP within this period are at the level of 60–120 microgram/ m^3 , as shown in Fig. 4a. The contribution of multiple-scattering events at the top of the mixing

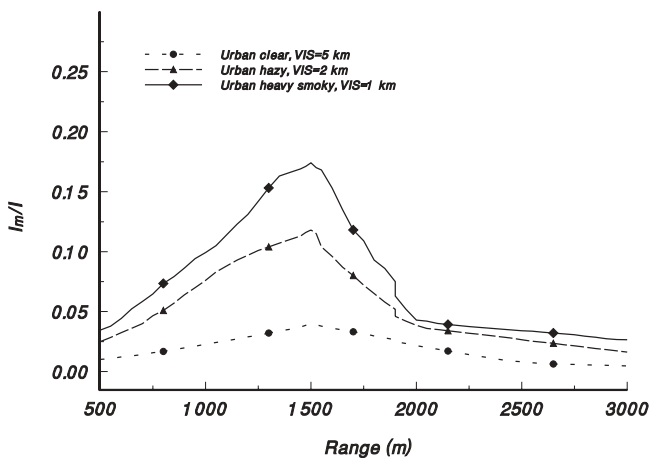
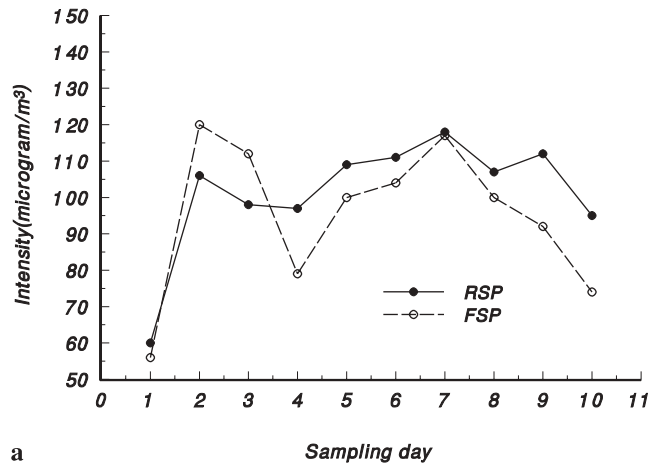
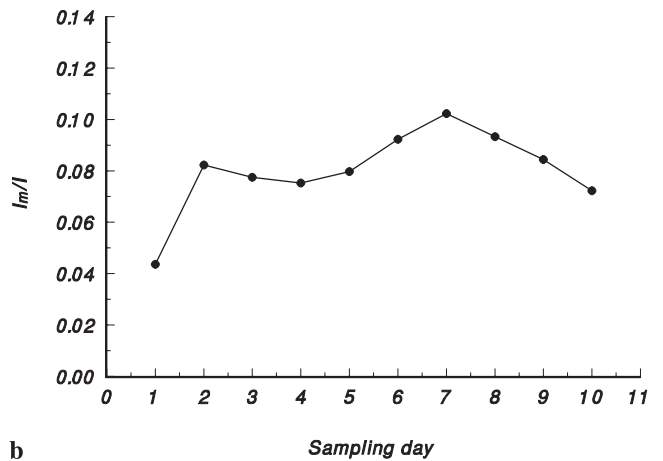


FIGURE 3 Contribution of multiply scattered photons to LIDAR returns estimated by Monte Carlo simulations for urban clear, urban hazy, and urban heavy smoke weather conditions



a



b

FIGURE 4 **a** Concentration of respirable suspended particulate (RSP) and fine suspended particulate (FSP) at 1400 LT for a period of ten days in Hong Kong urban areas. **b** Contribution of multiply scattered photons to LIDAR returns at the top of the mixing layer at 1400 LT for a period of ten days in Hong Kong urban areas

layer during the same period is calculated by the deconvolution model, and shown in Fig. 4b.

The influence of multiple scattering at the top of the mixing layer is related more closely to the concentration of RSP since the correlations between multiple scattering and RSP/FSP are 0.83 and 0.71, respectively. This comparison shows that the concentration of RSP plays an important role in LIDAR scattering problems in the local atmosphere, as a large concentration of RSP can produce more pronounced multiply scattered photons by building up more multiple-scattering events.

4 Summary

It was the objective of this study to analyze the influence of multiple scattering in ground-based SFOV LIDAR measurements. For this purpose LIDAR signals were calculated by means of time series deconvolution filtering models for different weather conditions.

The calculated LIDAR returns from urban clear, urban hazy, and urban heavy smoke atmospheres show the existence of multiple-scattering components in LIDAR returns. In particular, in the situation where the aerosol optical thickness is great, the contribution of multiple-scattering components to LIDAR returns may be as high as 14%; for a clear atmospheric condition where the aerosol optical thickness is small, such contributions are much lower, even under 5%.

Calculations by the time series deconvolution method are in good agreement with that by the Monte Carlo simulation method, indicating that the contribution of multiply scattered photons to LIDAR returns is strongly correlated with aerosol optical thickness. Comparison between deconvolution results and the concentration data of RSP/FSP observed by EPD also suggests that the concentration of respirable suspended particulate affects the laser scattering pattern in the local atmosphere of Hong Kong.

The advantage of this deconvolution method is that it does not need any prior knowledge of aerosol properties and

measurement geometries. The aerosol properties and measurement geometry are indispensable for Monte Carlo simulations, since the trajectories of scattering photons should be built up following given aerosol-distribution models. As such, the deconvolution method has much wider application potential in the situations where it is difficult to model aerosol distributions in the investigated atmosphere. Furthermore, the deconvolution algorithm is more efficient than Monte Carlo simulations, since multiple-scattering signals can be estimated within a few minutes, where it may need a few decades of computing time for Monte Carlo simulations.

REFERENCES

- 1 C.M.R. Platt: *J. Atmos. Sci.* **38**, 156 (1981)
- 2 P. Brusciaglioni, A. Ismaelli, G. Zaccanti: *Appl. Phys. B* **60**, 325 (1995)
- 3 L.R. Bissonnette, P. Brusciaglioni, A. Ismaelli, G. Zaccanti, A. Cohen, Y. Benayahu, M. Kleinman, S. Egert, C. Flesia, P. Schwendimann, A.V. Starkov, M. Noormohammadian, U.G. Oppel, D.M. Winker, E.P. Zege, I.L. Katsev, I.N. Polonsky: *Appl. Phys. B* **60**, 355 (1995)
- 4 J.D. Spinhrne: *Appl. Opt.* **21**, 2467 (1982)
- 5 K.E. Kunkel, J.A. Weinman: *J. Atmos. Sci.* **33**, 1772 (1976)
- 6 J. Ackermann, P. Völger, M. Wiegner: *Appl. Opt.* **38**, 5195 (1999)
- 7 D.L. Hutt, L.R. Bissonnette, L. Durand: *Appl. Opt.* **33**, 2338 (1994)
- 8 A.H. Hielscher, A.A. Eick, J.R. Mourant, I.J. Bigio: *Biomedical Sensing Imaging and Tracking Technologies II*, ed. by T. Va-Dinh, R.A. Lieberman, G.G. Vuvek [Proc. SPIE **2976**, 298 (1997)]
- 9 A.H. Hielscher, A.A. Eick, J.R. Mourant, D. Shen, J.P. Freyer, I.J. Bigio: *Opt. Express* **1**, 441 (1997)
- 10 G.E. Box, G. Jenkins: *Time Series Analysis, Forecasting and Control* (Holden-Day, San Francisco 1970)
- 11 K.J. Astrom, T. Bohlin: 'Numerical Identification of Linear Dynamic Systems from Normal Operating Records'. In: P.H. Hammond (Ed.): *Theory of Self Adaptive Systems* (Plenum, New York 1966)
- 12 G.C. Goodwin, R.L. Payne: *Dynamic System Identification: Experimental Design and Data Analysis* (Academic, New York 1977)
- 13 L. Bissonnette: *Appl. Phys. B* **60**, 315 (1995)
- 14 J.D. Klett: *Appl. Opt.* **20**, 211 (1981)
- 15 M. Hess, P. Koepke, I. Schult: *Bull. Am. Meteorol. Soc.* **79**, 831 (1998)
- 16 M.M. Raymond: *Laser Remote Sensing Fundamentals and Application* (Wiley InterScience, New York 1980) p. 73
- 17 W.E.K. Middleton: *Vision Through the Atmosphere* (University of Toronto 1958)